Annals of Nuclear Medicine Vol. 17, No. 7, 525–530, 2003

Evaluation of the number of SPECT projections in the ordered subsets-expectation maximization image reconstruction method

Yasuyuki TAKAHASHI,*,** Kenya MURASE,* Teruhito MOCHIZUKI,** Hiroshi HIGASHINO,***
Yoshifumi SUGAWARA** and Akiyoshi KINDA****

*Department of Medical Engineering, Division of Allied Health Sciences, Osaka University Graduate School of Medicine
**Department of Radiology, Ehime University School of Medicine
***Department of Radiology, Ehime Prefectural Imabari Hospital
****Toshiba Medical Engineering Laboratory

Filtered back projection (FBP) method, maximum likelihood-expectation maximization (ML-EM) method, and ordered subsets-expectation maximization (OS-EM) method are currently used for reconstruction of SPECT images in clinical studies. In the ML-EM method, images of good quality can be reconstructed even with a small sampling number of projection data, when compared with FBP. Shorter acquisition time and less radionuclide dose are preferable in the clinical setting if image quality is the same. In this study, we attempted to find optimal conditions for reconstruction of OS-EM images with commonly used sampling numbers of 30, 60 and 120 (step angles: 12°, 6°, and 3°, respectively), with acquisition counts/projection of 30, 60, 120 and 240 each. We adjusted the pixel counts of reconstructed images to be constant, by setting combination of sampling number and counts/projection (120 sampling number for 30 counts/projection, 60 for 60, and 30 for 120). Among the 3 acquisition conditions, the small sampling number of 30 had large acquisition counts per direction, resulting in low signal to noise ratio. Under this condition, the resolution was slightly low, but the uniformity of images was high. The combination of OS-EM and smaller sampling projection number may be clinically useful with reduction of the examination time, which is also beneficial to reduce dead time for gamma-camera rotation.

Key words: transmission computed tomography, ordered subsets-expectation maximization, the number of SPECT projections

INTRODUCTION

FILTERED BACK PROJECTION (FBP) method,[1] maximum likelihood-expectation maximization (ML-EM) method,[2,3] and ordered subsets-expectation maximization (OS-EM) method[4–6] are currently used for SPECT image reconstruction. There were 160 human studies in *The Journal of Nuclear Medicine* published between June 1997 and May 2002, 160 studies, in which the reconstruction methods, regions (head, myocardium, others), matrix sizes (64 × 64, 128 × 128, 256 × 256) and sampling angles (2°–12°) were all described (Fig. 1). Although FBP method was mostly used, ML-EM and OS-EM methods have also been used in the recent studies. In most studies using ML-EM and OS-EM methods, the sampling angle used was 3°[7] or 6°.[8] In general, better SPECT images are obtained with a larger number of sampling directions and with more acquisition counts/direction,[9] which requires the use of more radionuclide and/or longer acquisition time.

On the other hand, shorter acquisition time is beneficial for patient's tolerance and for reduction of radiation exposure. The OS-EM method suppresses deterioration of image quality even with small sampling numbers of projection data and with fewer acquisition counts. In this study, we performed simulation, phantom and human

Received March 31, 2003, revision accepted June 19, 2003.

For reprint contact: Yasuyuki Takahashi, Department of Health, Health Planning Division, Ehime Prefectural Matsuyama Regional Office, 132 Kita-Mochida, Matsuyama, Ehime 790–8502, JAPAN.

E-mail: takahashi-yasuyuki@pref.ehime.jp

studies to find optimal conditions for reconstruction of OS-EM images with commonly used sampling numbers of 30, 60 and 120.[10]

MATERIALS AND METHODS

SPECT system and data acquisition parameters

The triple headed SPECT system used was a GCA-9300A/UI (Toshiba Medical Systems, Tochigi, Japan) equipped with one cardiac fan beam collimator and two parallel beam collimators.[11] ^{99m}Tc was used as an external gamma-ray source for transmission CT (TCT) data. ^{99m}Tc myocardial was also used for SPECT data of phantom and human studies. The external gamma-ray source was a sheet-shape made from bellows tube, which was embedded in an acrylic rectangular board of 250 × 100 mm. The tube (1 mm in inner diameter) was made of fluorocarbon resin, and filled with 740 MBq of ^{99m}Tc. Data processor was a GMS-5500A/PI (Toshiba Medical Systems, Tochigi, Japan). Both TCT and SPECT images were sampled with a matrix size of 128 × 128, and the pixel size was 3.2 mm. In these conditions, the count per detector was about 75 counts/pixel in the myocardial phantom and was higher than 120 counts/pixel in the patient's myocardial area. Scatter correction was performed using the triple-energy window (TEW) method.[12] Acquisition window width of the TEW was 20% for the main window at 140 keV for ^{99m}Tc and 7% for the subwindow. TCT/ECT data were acquired with sequential mode.[13]

After truncation correction,[14] attenuation maps were generated from the TCT data using the filter back projection (FBP) methods.[7] Subsequently, parallel beam data of the 2 detectors for SPECT were summated. Then, SPECT images were reconstructed using OS-EM method (Subsets: 5, Iteration No. 10)[4–6] with TEW scatter correction.

The TCT projections were reconstructed with a ramp convolution filter, and high frequency noise was decreased with post-reconstruction Butterworth filtering (cutoff = 0.44 cycle/cm, power factor = 8).

Transverse SPECT images were reconstructed with a sampling number of 30, 60 and 120 and with counts/projection of 30, 60, 120 and 240 (240 counts/projection were not applied to studies of simulation, line source phantom, or human).

Simulation

By setting a SPECT value of 50 in a uniform circle (cylinder), projection data with 30, 60 and 120 counts at 360° were produced by Radon transformation.[15] The same SPECT value was applied to hot rods phantom. Images of the simulation were reconstructed taking the effects of the aperture of the parallel hole collimators into consideration.[16]

Line-source phantom study (FWHM)

Using ^{99m}Tc line source phantom (diameter, 1 mm), full width at half maxim (FWHM) was measured according to NEMA standard.[17] The rotation radius was 200 mm, and the sampling number was 30, 60 and 120, in which the maximum was 50 counts/pixel. Means of the measurements in center, transverse and long axial directions were calculated. Attenuation was not corrected.

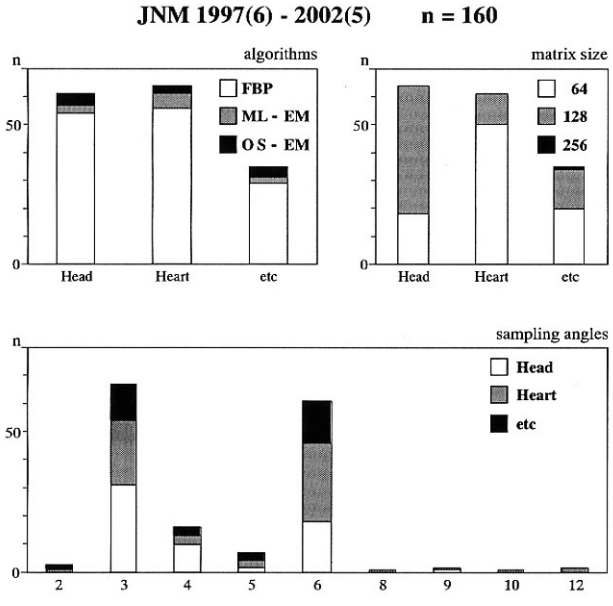

Fig. 1 Reconstruction methods, imaged regions, matrix sizes, and sampling angles were summarized form the 160 studies in *The Journal of Nuclear Medicine* published between June 1997 and May 2002.

Cylindrical (uniformity and hotrods) phantom

^{99m}Tc (92.5 kBq/m*l*) was filled in the cylindrical phantom (200 mmϕ × 200 mm circle, AZ-660, Anzai-Sogyo, Tokyo, Japan). The same radioactivity of ^{99m}Tc was filled in hot rods areas of the hot rods phantom. Images and profile curves of the various parameters were compared.

Myocardial phantom

Acquisition was performed after infusion of 92.5 kBq/m*l* into the myocardium of the phantom (Data Spectrum Corp., Hillsborough, NC) and 9.25 kBq/m*l* into the chest (background). The breasts were not created. Bull's eye maps were produced using a myocardial phantom in which a defect area (20 mm × 20 mm × 10 mm) had been established on the anterior wall.

Human study

TCT and ECT acquisition were performed in the sequential mode, separately.[13] The same ^{99m}Tc external source as the phantom studies was used for TCT data. After the TCT data, ECT data were acquired in a normal 36-year-old male 20 minutes after intravenous injection ^{99m}Tc-MIBI. The following 3 times with a sampling number of 30, 60 and 120 over 15 min. Dead-time for gamma-

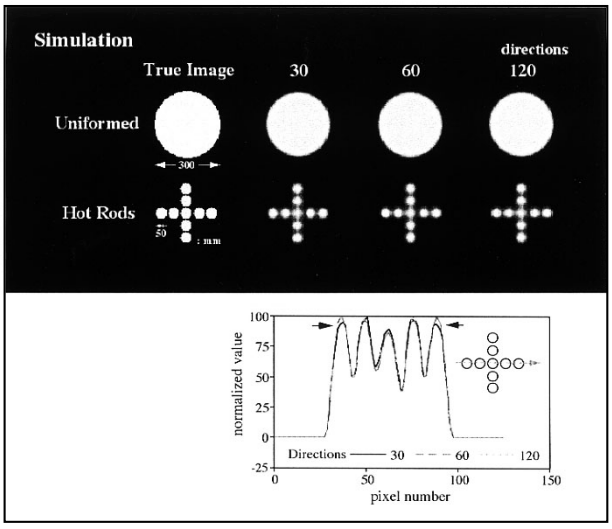

Fig. 2 Images were reconstructed with a sampling number of 30, 60 and 120 obtained by simulation (Radon transformation) of the numerical phantom as activity 50 and using additional information provided from the parallel hole collimators.
Graph: Profile curve of the hot rods phantom used for the simulation.

camera rotation was not included in the 15 min. To avoid misregistration between TCT and ECT data, he did not move until both data acquisitions were completed.

Data analysis

Images obtained from a cylindrical phantom with the same number of acquisition counts were used for comparisons. Profile curves were used for the evaluation of the uniformity, and shown by normalizing the maximum of each ECT image to 100%.

In the experiments using a myocardial phantom, the normalized root mean square error (NRMSE (%), $\sqrt{\Sigma(X_i - O_i)^2/\Sigma O_i^2} \times 100$; X_i, measurement image; O_i, standard image; i, pixel number ($i = 1 - n$))[18] was determined

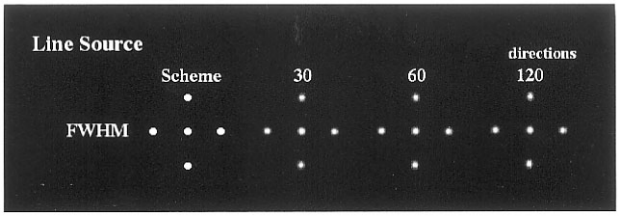

Fig. 3 The images in the bottom were obtained from a line-source phantom with a sampling number of 30, 60 and 120 to measure FWHM.

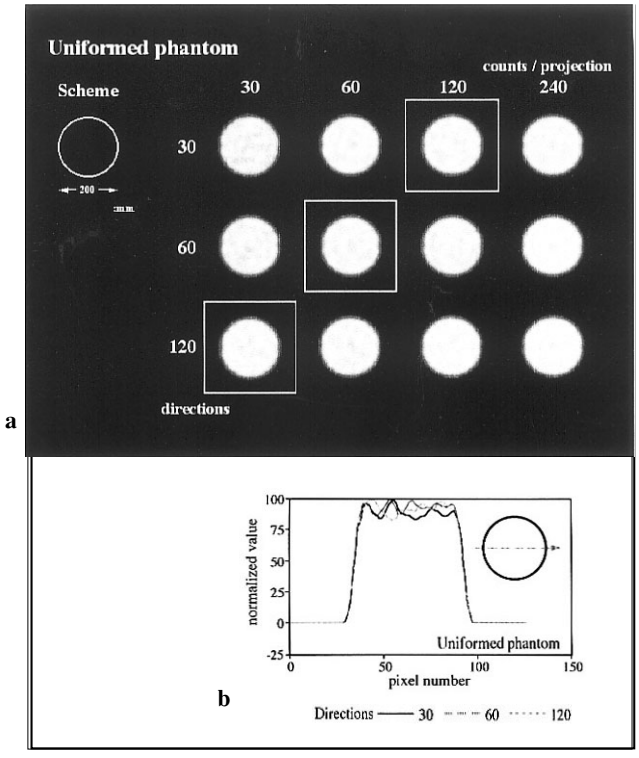

Fig. 4 (a) SPECT images for the evaluation of the uniformity with changes in the sampling number (30, 60, 120) and acquisition counts (30, 60, 120, 240) in the ^{99m}Tc cylindrical phantom. (b) Profile curves of the uniformity in the cylindrical phantom.

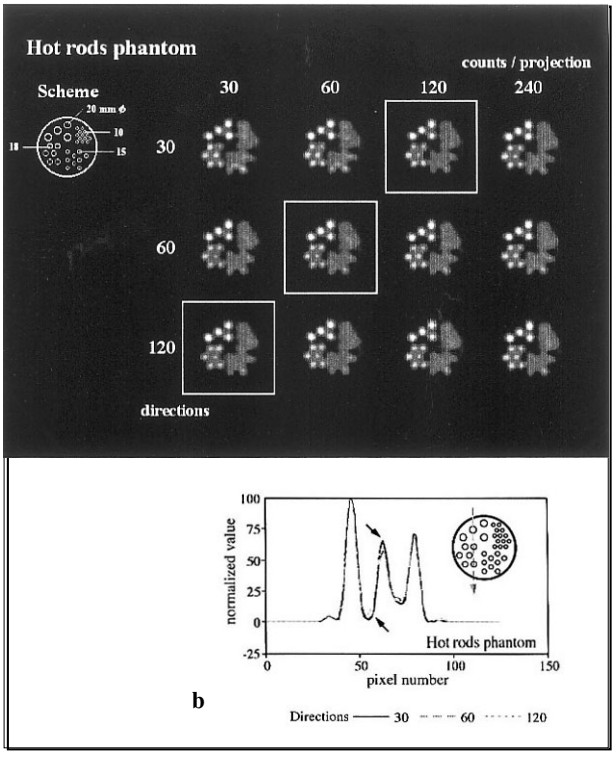

Fig. 5 (a) SPECT images for evaluation of imaging quality of hot rods with changes in the sampling number (30, 60, 120) and projection counts (30, 60, 120, 240) in the ^{99m}Tc cylindrical phantom. (b) Profile curves of the uniformity in the cylindrical phantom.

Table 1 A sampling number of 30, 60 and 120 compare the SPECT image of, uniformed phantom, hot rods phantom (maximum and minimum values) and human study (septum and cavity values), and FWHM and SPECT values are shown

sampling numbers	FWHM (mm)	SPECT values				
		phantom study			human study	
		Uniformed	hot rods		myocardium	
		Mean ± SD (CV%)	Maximum	Minimum	Septum	Cavity
30	12.95	95.44 ± 3.84 (4.02)	66.11	17.88	65.77	30.46
60	12.89	94.17 ± 4.26 (4.52)	61.41	17.07	78.30	40.89
120	12.76	92.76 ± 4.59 (4.95)	57.26	15.83	57.42	35.95

Table 2 NRMSE (%) in the images with various sampling numbers and acquisition counts calculated using the image obtained from the myocardial phantom with the sampling number of 120 and 240 counts/projection as the standard

NRMSE (%)		counts/projection			
		30	60	120	240
sampling numbers	30	4.87	4.01	3.82	3.17
	60	4.67	3.78	3.39	2.51
	120	4.50	3.55	2.66	—

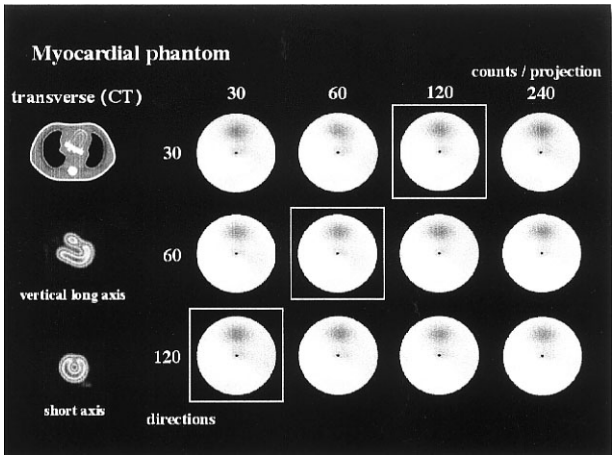

Fig. 6 Bull's eye images with different sampling numbers (30, 60, 120) and projection counts (30, 60, 120, 240) in the ^{99m}Tc myocardial phantom.

using images with 240 counts/projection at a sampling number of 120 with the largest number of counts as the standard.

The contrast of the SPECT value (maximum) on the lateral wall of myocardium was regarded as 100 in the human study, and the profile curves (arrows shown in the schemes of Fig. 7) of transverse images were produced for comparisons.

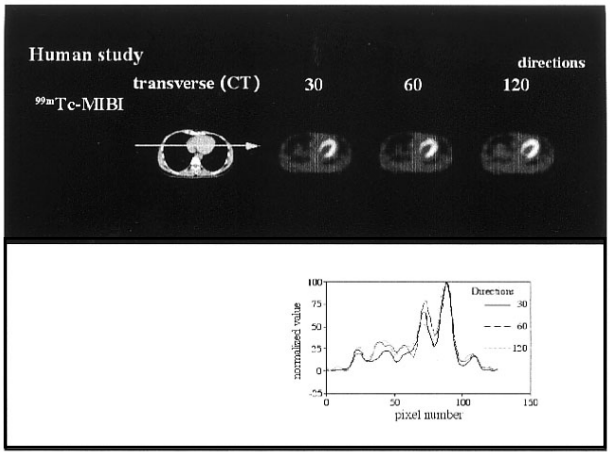

Fig. 7 ^{99m}Tc-MIBI myocardial SPECT images in the human study. Imaging was performed 3 times with a sampling number of 30, 60 and 120 for a fixed time excluding the time required for moving the gamma camera.

RESULTS

Simulation study

There were no significant differences in the uniformity among the sampling numbers (Fig. 2). However, the contrast of the second right and the second left rods (%) with the sampling number of 30 was 10% lower in the first right and the first left rods than that with the sampling number of 120.

Line-source phantom study (FWHM)

FWHM in the sampling numbers of 30, 60 and 120 are shown in Table 1 (not significant) (Fig. 3).

Cylindrical (uniformity and hot rods) phantom

The uniformed images and profile curves along a line are shown in Figure 4 (a) and Figure 4 (b). The normalized SPECT values (mean ± SD [CV%]) on the internal side at both ends of the transaxial image are shown in Table 1, indicating that it was stable even with a sampling number of 30.

The hot rods images and profile curves along of the

center rods are shown in Figure 5 (a) and Figure 5 (b). The normalized SPECT values in the maximum and minimum areas are shown in Table 1, indicating that it was visualized most clearly with a sampling number of 120.

Myocardial phantom

The NRMSE (%) determined using the myocardial phantom was reduced with the increase in the sampling number and acquisition time (Fig. 6, Table 2). The errors in all images were within 5%.

Human study

In the normal volunteer, normalized SPECT values of interventricular septum and cardiac cavity in the profile curves of the transaxial image (Fig. 7) are shown in Table 1. Interventricular septum was visualized most clearly with the sampling number 60. The minimum SPECT values in the cardiac lumen was lowest with the sampling number of 30.

DISCUSSION

In this study, we examined the relation between the sampling numbers of the projection and the SPECT images quality. With regard to the sampling number and resolution, an equation, $N = \pi \times D$ (diameter of the field of view, mm)/2a (pixel size, mm), is proposed and generally accepted.[19] Using this equation, a matrix of 128×128 and a sampling number of 200 were required in the present study performed with an effective visual field of 410 mm and a pixel size of 3.2 mm (acquisition magnification, 1). We evaluated the applicability of this equation to the SPECT apparatus equipped with collimators by simulation, and found that there were no differences with the number of counts obtained in clinical images, indicating that the equation cannot be necessarily applied in the clinical SPECT images.

We examined the effects of the sampling number on the uniformity. There were no differences in the uniformity among the sampling numbers when total acquisition counts were same, suggesting that good ECT images are obtained with sufficient acquisition counts per direction even though the sampling number is small, i.e., with less signal to noise per direction.

We also examined which is more important, the sampling number or acquisition counts, in the image quality, using the data obtained from the myocardial phantom study and human study. When the similar imaging counts were used, there were no differences among the sampling numbers. However, considering the dead-time for gamma camera rotation, 120 sampling required the longest the examination time unless the continuous mode acquisition[20] was not applied. Thus, total acquisition time including dead time for rotation was considered, image quality obtained with the sampling time of 120 may be poor compared with images of the other sampling number. Acquisition counts should be considered more important than the sampling number in SPECT with small acquisition counts such as ^{123}I-MIBG.[21]

Long time was required to obtain ECT images reconstructed by ML-EM. However, with the development of the OS-EM method and with the spread of work stations by which faster calculation is possible, reconstruction of images has become possible in the clinical setting. Its principle guarantees convergence of reconstructed images even with a small number of acquisition counts and a small sampling number, and aliasing artifacts[22] observed in images reconstructed by the FBP method are not observed with OS-EM, suggesting that the sampling number can be reduced to a certain level. If the sampling number is excessively small, the image quality might be reduced as shown in the data of the cardiac cavity by the studies of hot rods and human study.

CONCLUSION

We examined the effects of the sampling number on images reconstructed by the OS-EM method. The comparisons of reconstructed images obtained with a sampling number of 120 and 30 counts/projection, with 60 and 60, and with 30 and 120 indicated that the image quality as judged from the uniformity and resolution was generally higher with a smaller sampling number and a larger number of counts/projection. Considering the dead time for rotation of the gamma camera, this acquisition method with OS-EM will be clinically useful with reduction of the examination time.

ACKNOWLEDGMENT

The authors thank Mr. Shin-nosuke Yasuhisa, Mr. Toshizumi Kikuchi and Mr. Kenji Kariya (Daiichi Radioisotope Labs., Ltd.) and Mr. Hiroshi Miguchi (Ehime Prefectural Imabari Hospital), and Mr. Hiroyuki Shinbata, Mr. Akira Masuhara (Ehime Prefectural Central Hospital), and Mr. Matsutarou Hamada, Mr. Katsuhito Itou (Ehime Prefectural Niihama Hospital) for their technical support.

REFERENCES

1. Ramachandran GN, Lakshminarayanan AV. Three-dimensional reconstruction from radiographs and electron micrographs: Applications of convolutions instead of Fourier transforms. *Proc Natl Acad Sci Amer* 1971; 68: 2236–2240.
2. Sheep LA, Vardi Y. Maximum likelihood reconstruction for emission tomography. *IEEE Trans Med Imag* 1982; MI-1: 113–122.
3. Murase K, Tanada S, Inoue T, Sugawara Y, Hamamoto K. Improvement of brain single photon emission tomography (SPECT) using transmission data acqusition in a four-head SPECT scanner. *Eur J Nucl Med* 1993; 20: 32–38.
4. Hudson HM, Larkin RS. Accelerated image reconstruction using ordered subsets of projection data. *IEEE Trans Med*

Imaging 1994; MI-13: 601–609.
5. Murase K, Tanada S, Sugawara Y, Tauxe WN, Hamamoto K. An evaluation of the accelerated expectation maximization algorithms for single-photon emission tomography image reconstruction. *Eur J Nucl Med* 1994; 21: 597–603.
6. Takahashi Y, Murase K, Higashino H, Sogabe I, Sakamoto K. Receiver operating characteristic (ROC) analysis of image reconstructed with iterative expectation maximization algorithms. *Ann Nucl Med* 2001; 15: 521–525
7. Araujo LI, Jimenez-Hoyuela JM, McClellan JR, Lin E, Viggiano J, Alavi A. Improved uniformity in tomographic myocardial perfusion imaging with attenuation correction and enhanced acquisition and processing. *J Nucl Med* 2000; 41: 1139–1144.
8. Ficaro EP, Fessler JA, Ackemann RJ, Rogers WL, Corbett JR, Chwaiger M. Simultaneous transmission-emission thallium-201 cardiac SPECT: Effect of attenuation correction on myocardial tracer distribution. *J Nucl Med* 1995; 36: 921–931.
9. Kojima A, Matsumoto M, Takahashi M, Hirota Y, Yoshida H. Effect of spatial resolution on SPECT quantification values. *J Nucl Med* 1989; 30: 508–514.
10. Fukuchi K, Sago M, Nitta K, Fukushima K, Toba M, Hayashida K, et al. Attenuation correction for cardiac dual-head γ camera coincidence imaging using segmented myocardial perfusion SPECT. *J Nucl Med* 2000; 41: 919–925.
11. Ichihara T, Motomura N, Ogawa K, Hasegawa H, Hashimoto J, Kubo A. Evaluation of SPECT quantification of simultaneous emission and transmission imaging of the brain using a multidetector SPECT system with the TEW scatter compensation method and fan-beam collimation. *Eur J Nucl Med* 1996; 23: 1292–1299.
12. Ogawa K. Simulation study of triple-energy-window scatter correction in combined Tl-201, Tc-99m SPECT. *Ann Nucl Med* 1995; 8: 277–281.
13. Vidal R, Buvat I, Darcourt J, Migneco O, Desvignes P, Baudouy M, et al. Impact of attenuation correction by simultaneous emission/transmission tomography on visual assessment of ^{201}Tl myocardial perfusion images. *J Nucl Med* 1999; 40: 1301–1309.
14. Motomura N, Ichihara T, Takayama T, Nishihara K, Inouye T, Kataoka T, et al. Practical method for reducing truncation artifacts in a fan beam transmission CT system. *J Nucl Med* 1998; 25 (Suppl): p178.
15. Radon J. On the determination of functions from their integrals along certain manifolds. *Mathematisch-Physische Klasse* 1917; 69: 262–277.
16. Anger HO. Scintillation camera with multichannel collimator. *J Nucl Med* 1964; 5: 515–531.
17. National Electrical Manufacturers Association. Performance Measurements of Scintillation Camera NEMA standards Publication No. NU1-1994; 1994.
18. Takahashi Y, Murase K, Higashino H, Mochizuki T, Motomura N. Attenuation correction of myocardial SPECT images with X-ray CT: Effects of registration errors between X-ray CT and SPECT. *Ann Nucl Med* 2002; 16: 431–435.
19. Larsson SA. Gamma Camera Emission Tomography. Acta Radiologica Stockholm, 1980; 21–22.
20. Cao Z, Maunoury C, Chen CC, Holder LE. Comparison of continuous step-and-shoot versus step-and-shoot acquisition SPECT. *J Nucl Med* 1996; 37: 2037–2040.
21. Nakajima K, Bunko H, Taki J, Shimizu M, Muramori A, Hisada K. Quantitative analysis of ^{123}I-meta-iodobenzylguanidine (MIBG) uptake in hypertrophic cardiomyopathy. *Am Heart J* 1990; 119: 1329–1337.
22. Cao Z, Holder LE, Chen CC. Optical number of views in 360° SPECT imaging. *J Nucl Med* 1996; 37: 1740–1744.